

RESEARCH

Open Access



Protective mechanism of safflower yellow injection on myocardial ischemia-reperfusion injury in rats by activating NLRP3 inflammasome

Lingmei Li^{1†}, Ce Cao^{2†}, Hao Guo², Li Lin², Lei Li², Yehao Zhang², Gaojie Xin², Zixin Liu², Shujuan Xu², Xiao Han^{2*}, Qiong Zhang^{2*} and Jianhua Fu^{2*}

Abstract

Objectives This study intended to explore whether the protective effect safflower yellow injection (SYI) on myocardial ischemia-reperfusion (I/R) injury in rats mediated of the NLRP3 inflammasome signaling.

Methods The I/R model was prepared by ligating the left anterior descending coronary artery for 45 min and then releasing the blood flow for 150 min. 96 male Wistar rats were randomly divided into sham group, I/R group, Hebeishuang group (HBS), SYI high-dose group (I/R + SYI-H), SYI medium-dose group (I/R + SYI-M) and SYI low-dose group (I/R + SYI-L). Cell experiments were divided into normal control group (NC), Oxygen glucose deprivation/reoxygenation group (OGD/R), OGD/R + SYI group, OGD/R + SYI + Chloroquine group (OGD/R + SYI + CQ). The area of myocardial ischemia infarction and pathological changes were observed by the Tetrazolium method (TTC) and HE staining. Myocardial enzymes such as aspartate aminotransferase (AST), lactate dehydrogenase (LDH) and creatine kinase (CK) were measured by chemiluminescence (CL) method. The inflammatory factors levels of TNF- α , IL-1 β , MCP-1, and IL-6 were detected by ELISA. The expressions of inflammatory-related proteins (Caspase-1, NLRP3, TLR4, NF- κ B), autophagosome-related proteins (LC3-I, LC3-II, LC3-II/LC3-I), apoptosis-related proteins (Bax, Bcl-2, Caspase-3, Bcl-2/Bax) and autophagy-related proteins (p62/SQSTM1, PI3K, p-Akt, mTOR) were detected by Western-Blot. Cell morphology and cell viability were detected by transmission electron microscopy and CCK-8.

Results In vivo, compared with sham group, the percentage of myocardial infarction area was increased and myocardial tissue arrangement was disordered in I/R group. In addition, the activities of myocardial enzymes, the contents of inflammatory factors, the expressions of inflammatory-related proteins, autophagy-related proteins,

[†]Lingmei Li and Ce Cao contributed equally to this work.

*Correspondence:

Xiao Han

hxfresh@sina.com

Qiong Zhang

zhangq810@263.net

Jianhua Fu

jianhuaaffcn@263.net

Full list of author information is available at the end of the article



autophagosome-related proteins, Bax and Caspase-3 were increased, while Bcl-2 and Bcl-2/Bax were decreased. SYI treatment reversed these trends, except for the expression of autophagosome-related proteins. In vitro, SYI decreased the contents of inflammatory factors and the expressions of inflammatory-related proteins, autophagy-related proteins and autophagosome-related proteins caused by OGD/R. However, the contents of inflammatory factors and the expression of inflammatory-related proteins, p62/SQSTM1 and mTOR were increased, while PI3K, p-AKT, LC3-II/LC3-I were significantly decreased in OGD/R + SYI + CQ group.

Conclusions SYI can promote myocardial tissue autophagy by regulating NLRP3, thereby attenuating the myocardial inflammatory response and protecting damaged myocardium in I/R rats.

Keywords Safflower yellow injection, Myocardial ischemia-reperfusion injury, Inflammation, Autophagy, NLRP3

Introduction

Coronary artery disease (CAD), which is known as the “top killer” that endangers human health, remains the leading cause of death around the world. Restoring blood perfusion is the most effective and important way to treat CAD. However, a large number of studies have shown that ischemic myocardial tissue restores blood supply, which can further damage myocardial tissue and affect myocardial fiber structure, electrophysiological function, and myocardial metabolic function, thereby weakening the efficacy of coronary revascularization therapy, which was called myocardial ischemia-reperfusion injury (MIRI) [1–5]. Relevant studies have shown that MIRI-damaged myocardium can even account for 50% of the total infarcted myocardial area [6–8]. Among them, the inflammatory response, which is one of the key pathological mechanisms in the process of MIRI, runs throughout the whole process of myocardial injury and repair after ischemia-reperfusion, besides, it is also a key factor and an important target that determines the final myocardial infarction size and adverse myocardial remodeling point. During the initial stage of MIRI, the danger signal is recognized by the recognition receptors on the inflammasome and activates the inflammasome, which will stimulate the endogenous inflammatory response of cardiomyocytes and induces vascular endothelial cells and fibroblasts to generate a large number of pro-inflammatory factors, causing severe damage to cardiomyocytes [9–11]. Although early reperfusion therapy for acute myocardial infarction can effectively salvage ischemic myocardium, a considerable portion of cardiomyocytes may still occur irreversible necrosis and loss, which compromises the long-term survival of patients with myocardial infarction.

A variety of inflammatory factors are involved in MIRI. TNF- α greatly increases the infiltration of granulocytes into the ischemia-reperfusion area by promoting the adhesion and interaction of leukocytes and endothelial cells, resulting in myocardial damage [12]. IL-6 has long been considered to be a cytokine involved in the acute phase response, and its expression is significantly elevated in ischemia-reperfusion myocardium [13]. IL-1 β

downregulates calcium-operating protein in ischemic cardiomyocytes, reduces L-type channel calcium current, induces calcium leakage from the sarcoplasmic reticulum, and leads to myocardial contractile dysfunction [14]. Moreover, IL-1 β can also increase nitric oxide production by up-regulating inducible nitric oxide synthase (iNOS), leading to cardiomyocyte apoptosis and tissue remodeling [15]. Therefore, IL-1 β is a key factor regulating the inflammatory response. It is involved in the recruitment of immune cells and provides the necessary conditions for the subsequent production of other pro-inflammatory factors. Given the important role of IL-1 β in the inflammatory response, modulating the production of IL-1 β could significantly reduce MIRI.

NLRP3 can induce the production of IL-1 β by activating the protein of caspase-1. In ischemia-reperfusion myocardial tissue, the protein expression levels of NLRP3 and ASC were significantly increased [16]. A cascade of cellular inflammatory responses will be led by the activation of the inflammasome and release of IL-1 β , which leads to the generation of more endogenous danger signals and the amplification of inflammatory signals, resulting in the adhesion of neutrophils and monocytes and the generation of free radicals [16]. NLRP3 can be activated by many different endogenous and exogenous factors. TLR ligands can induce NF- κ B activation and up-regulate the transcription and protein expression of NLRP3 [17]. NLRP3 is then activated by different mechanisms to assemble with ASC and caspase-1 to form an inflammasome, resulting in the cleavage and release of mature IL-1.

In the inflammatory response, autophagy is one of the important mechanisms to negatively regulate the activation of the NLRP3 inflammasome. As the key factor in the activation of NLRP3, ROS are mainly produced by mitochondria. When organisms are stimulated by outside, mitochondria will be damaged and gradually accumulated in cells, resulting in a large accumulation of ROS. Moreover, autophagy is an important way for cells to clear damaged mitochondria, reduce ROS accumulation, and maintain normal mitochondrial function, which also plays an important role in the MIRI process.

Previous studies have shown that mTOR inhibitors can induce autophagy, and inhibit AKT phosphorylation, thereby reducing mitochondrial ROS production and IL-1 β secretion. This suggests that drugs can induce autophagy and negative feedback regulate the activation of the NLRP3 inflammasome, thereby reducing the secretion of IL-1 β and reducing the inflammatory response, which has become a key strategy for the treatment of the MIRI. The activation of the NLRP3 inflammasome and its downstream inflammatory signaling molecules is the main way to induce the inflammatory response after myocardial ischemia [18].

Safflower Yellow Injection (SYI) is an injection of water-soluble component of traditional Chinese medicine safflower (*Carthamus tinctorius* L.), which contains hydroxy safflower yellow A (HSYA), anhydrosafflor yellow B (AHSYB), quercetin, kaempferol and other flavonoids. SYI, which is mainly used for the treatment of CAD, angina pectoris and other diseases, can effectively reduce the levels of serum inflammatory factors in patients with coronary heart disease and angina pectoris, but its anti-inflammatory mechanism is not fully understood [19]. The previous study of our group found that Safflower Yellow has significant anti-inflammatory and anti-myocardial ischemic effects [20, 21], and found that the anti-inflammatory effect of HSYA is related to its activation of autophagy and regulation of NLRP3 inflammasome [22]. Therefore, we aimed to investigate whether the effect of SYI on MIRI in rats is related to its regulation of the anti-inflammatory signaling pathway of the NLRP3 inflammasome, and explore the regulatory mechanism of autophagy on the NLRP3 inflammasome, thus verifying the mechanism of action of SYI against MIRI and providing an experimental basis for SYI in the prevention and treatment of CAD.

Materials and methods

Animals and cells

Ninety-six SPF grade male healthy adult Wistar rats (200–240 g, 7 weeks old) were obtained from SiPeiFu (Beijing) Biotechnology Co., Ltd. [Animal certificate number: SCXK (Beijing) 2016-0002]. These rats were given chow and water-adapted feeding for 3 days and were randomly divided into 6 groups with 16 rats in each group, namely Sham group, I/R group, SYI high-dose group (32 mg·kg⁻¹), SYI medium-dose group (16 mg·kg⁻¹), SYI low-dose group (8 mg·kg⁻¹) and Hebeishuang group (1 mg·kg⁻¹). Drug doses were determined by reference to previous literature [23–25]. Before the operation, the medicine was formulated into the required concentration with physiological saline. After the left anterior descending coronary artery was threaded, the rats in each group were injected medicine (3 mL·kg⁻¹) once through the tail vein immediately, except the Sham

group and the I/R group were injected with the physiological saline. The ethics committee of Xiyuan hospital approved the study (No.2021XLC037, March 29 2021).

Human umbilical vein endothelial cells (HUVECs) were purchased from Procell Life Science&Technology Co., Ltd. (Lot: CL-0122). The experiment was divided into the normal control group (NC), Oxygen-Glucose Deprivation/Reoxygenation group (OGD/R), OGD/R+SYI (35 $\mu\text{g}\cdot\text{mL}^{-1}$) group (OGD/R+SYI), OGD/R+SYI+chloroquine (50 $\mu\text{mol}\cdot\text{L}^{-1}$) group (OGD/R+SYI+CQ). The dose of chloroquine was determined by reference to previous literature [26–28].

Establishment of animal model

The establishment of the animal model was based on previous literature and refined according to the pre-testing and previous experimental experience of the research group [29–32]. Wistar rats were anaesthetized with 1% sodium pentobarbital (50 mg/kg) by intraperitoneal anesthesia and connected to the small-animal ventilator for artificial respiration and the small-animal electrocardiograph. Anesthesia was complete when muscle tension, corneal reflexes and response to skin pinching disappeared in the rats. The chest was then opened and the pericardium exposed by breaking the 3–4 ribs. Once the heart was exposed, a suture was placed approximately 2 mm below the bifurcation of the left anterior descending coronary artery and the drug/physiological saline was immediately injected through the tail vein. After stabilization for 10 min, the silk thread was threaded with a small polyethylene tube, tightening the silk thread, causing myocardial ischemia by pushing the tube method. The judgment criteria for ischemia success were adopted by using the electrocardiogram QRS amplitude to increase, ST-segment elevation and T wave towering or inversion. After 45 min of the chest was closed, the silk thread was cut to realize the reperfusion process. Meanwhile, the chest wall was sutured and the animals resumed spontaneous breathing. After 150 min of reperfusion, the rats were anesthetized, and blood and myocardial tissue samples were collected and stored for examination. Notably, the sham operation group only threading without ligation, and other operations were the same as the model group.

Establishment of cell model

The HUVECs were inoculated in a 96-well plate or a clear sterile plastic petri dish with Lids then put in the cell incubator with a 37 °C, 5% CO₂ for 24 h. After discarding the old medium and washing with PBS for 2–3 times, in the NC group, the old medium was replaced with DMEM complete medium, and put the 96-well plate or the clear sterile plastic petri dish with Lids back in the incubator for 6 h waiting for testing. Meanwhile,

after washing the old medium in the OGD/R group and each administration group, the old medium was replaced with an N₂-saturated sugar-free medium in the OGD/R group, and N₂-saturated drug-free sugar-free medium in each administration group. In an airtight box, continuously flowing 950 mL·L⁻¹ N₂ + 50 mL·L⁻¹ CO₂ mixed gas for 30 min to fully exhaust the residual oxygen, consequently, the cells were cultivated in the cell incubator for 4 h. After the end of 4 h, the airtight box was opened and the 96-well plate or the clear sterile plastic petri dish with Lids was taken out, moreover, the sterile glucose solution was added to make the glucose concentration in the culture medium of 4.5 g/L. Cell viability was detected by cell-counting-kit-8 after the 96-well plate or the clear sterile plastic petri dish with Lids was placed back in the incubator for 2 h.

Determination of SYI composition and content

The ingredients indicate that every 150 mg of safflower yellow for injection contains 80 mg of total safflower ketone. However, the specific ingredients and content of SYI are unknown, therefore, we carried out qualitative and quantitative research on the main components of safflower pigment for injection, and carried out the mass spectrometry characteristics of possible compounds by liquid chromatography-mass spectrometry, mainly for quercetin, hesperidin, rutin, luteolin, isorhamnetin, luteolinluco side, isoquercitrin, apigenin-7-O-beta-D-glucoside, apiin, hydroxysafflor A, anhydrosafflor yellow B and Baicalin was analyzed. A high-sensitivity analytical method for the above compounds was constructed, and on this basis, the chromatographic conditions were explored to determine which components they contained, and HPLC fingerprint technology was used to carry out quantitative analysis and research to clarify the content of the main components, to further study the mechanism of SYI.

HE Staining of myocardial tissue

After reperfusion, the rats were anesthetized by intraperitoneal injection of sodium pentobarbital. Subsequent experiments were performed after the rats were put under deep anesthesia. The thickness of 4 mm cardiac tissue was cut from the heart cross-section below the ligation line and fixed with 4% formalin for 24 h. Subsequently, the thick 4 mm cardiac tissue was embedded in paraffin, and HE staining was used to observe the pathological changes in myocardial tissue.

Measurement of myocardial infarct size by TTC staining

After the end of reperfusion, the rats were anesthetized by intraperitoneal injection of sodium pentobarbital. At the same time, the heart was quickly taken out and blotted dry with filter paper, and then placed in a -20 °C

refrigerator for quick freezing for about 10 to 15 min. 5 uniform slices with a thickness of about 1 mm were cut from the heart, and then the slices were quickly placed in a 6-well plate containing TTC staining solution and incubated at 37 °C for 15–30 min in the dark. After the color development of the section is completed, the slices were placed in a special solution for some time in 10% formalin to increase the contrast. After that, the stained tissues were taken out and rinsed with normal saline to an off the excess staining solution on the surface of the tissue. Image J was used to measure and analyze the infarct size and total myocardial area (percentage of infarct area = total infarct area/total myocardial area × 100%).

Detection of serum myocardial enzymes and inflammatory factors

After the reperfusion was completed, the rats were anesthetized by intraperitoneal injection of sodium pentobarbital. The blood was collected from the abdominal aorta, left standing at room temperature for 1 h, and centrifuged at 3500 rpm for 10 min in order to separate the serum. Adding and mixing a certain amount of PBS to the cell pellet, after the cells were suspended in PBS, the cell suspension was transferred to a glass homogenization tube in the ice-water mixture. Manually homogenizing for 3 min, the broken cell suspension can be used for measurement. After taking the serum sample and preparing reagents according to the instructions of AST, CK, and LDH kits and mixing the reagents with animal serum samples in proportion, the contents of AST, CK, and LDH were calculated by detecting the absorbance values of the sample at 660 nm, 505 nm, or 450 nm by a microplate reader. Meanwhile, according to the instructions of the ELISA kit, a standard curve was drawn to detect the contents of inflammatory factors TNF-α, IL-6, MCP-1, and IL-1β when the microplate reader was used to detect the absorbance value of the serum sample or cell suspension.

Western blot analysis

To obtain the protein of rat myocardial tissue, after reperfusion, the rats were anesthetized by intraperitoneal injection of sodium pentobarbital. The ischemic and peripheral myocardial tissue were collected under the ligation and cut into pieces with surgical scissors. The tissue cells were lysed with RIPA lysis buffer (containing protease inhibitors and phosphatase inhibitors). In order to obtain the protein of HUVECs, adding and mixing a certain amount of PBS to the cell pellet, after the cells were suspended in PBS, the cell suspension was transferred to a glass homogenization tube in the ice-water mixture. Manually homogenizing for 3 min, the broken cell suspension can be used for measurement. The protein was transferred to the PVDF membrane by determining

the concentration by BCA protein detection kit. The membranes were incubated with the primary antibodies against mTOR, PI3K, p62, NLRP3, NF- κ B, P-Akt, Caspase-3, Caspase-1, LC3, TLR4, IL-1 β , IL-6, MCP-1, TNF- α , Bcl-2, Bax and β -actin overnight at 4 °C. Then, the membranes were washed with TBST buffer and incubated with secondary antibody in TBST buffer at 37 °C for 1 h. Finally, the membranes were washed and visualized using Super ECL Western Blotting Substrate, and the bands were scanned and quantified using the ImageJ system.

Cell viability assay

After each treatment, Cell Counting Kit-8 was used to measure the viability of HUVECs according to the standard protocol of the manufacturer. The absorbance was determined at 450 nm using a spectrophotometer.

Experimental instruments

API4000QTRAP mass spectrometer system, equipped with ESI ion source and Analysis1.5.1 data processing system, purchased from Applied Biosystems, Inc (USA). ICE-CL31R cryogenic centrifuge, Ultra-low temperature refrigerator and Spectrophotometer (NANODROP2000) were purchased from Thermo Fisher Scientific (USA). ALC-V8 small animal ventilator was purchased from Shanghai Alcott Biotechnology Co., Ltd. (China). MPIAS-500 Multimedia Color Pathology Graphic Analysis System was purchased from Jingzheng Hengbocheng Technology Development Co., Ltd. (China). The microplate reader (BioTekSYNERGY4) was purchased from Berten Instrument Co., Ltd. (USA). Biological signal acquisition and processing system (BL-420 F) was purchased from Sichuan Chengdu Taimeng Technology Co., Ltd. (China). Electrophoresis instrument (powerpac200) was purchased from Bio-Rad Laboratories, Inc. (USA). Hitachi Transmission Electron Microscope (H-7500) was purchased from Hitachi Limited (Japan). The Gel imaging system (Tanon1600) was purchased from Shanghai Tianneng Technology Co., Ltd. (China).

Reagents and antibodies

Safflower yellow pigment for injection was purchased from Shanxi Deyuantang Pharmaceutical Co., Ltd., (lot No.713020334391, China). Hebeishuang (Diltiazem) was purchased from Tianjin Tanabe Pharmaceutical Co., Ltd. (lot No.B014, China). Autophagy inhibitor, chloroquine, was purchased from Sigma-Aldrich Co., Ltd. (lot No.095m14016V, USA). Anti-Caspase-3 antibody (Cat No.ab13847), Anti-LC3 (Cat No.ab51520), Anti-P62 (Cat No.ab56416), Anti-TLR4 (Cat No.ab13867), Anti-mTOR (Cat No.ab32028), Anti-PI3K (Cat No.ab151549) and Anti-NLRP3 (Cat No.ab214185) were purchased from Abcam Plc (United Kingdom). Anti-GAPDH antibody

(Cat No.5174), Anti-NF κ B antibody(p65) (Cat No.8242) and Anti-AKT (Cat No.4060) were purchased from Cell Signaling Technology (USA). Anti-Caspase-3 antibody (Cat No.ab13847), Anti-LC3 (Cat No.ab51520), Anti-P62 (Cat No.AB56416), Anti-TLR4 (Cat No.ab13867), Anti-mTOR (Cat No.ab32028), Anti-PI3K (Cat No.ab151549) and Anti-NLRP3 (Cat No.ab214185) were purchased from Abcam Plc (United Kingdom). Anti-GAPDH antibody (Cat No.5174), Anti-NF κ B antibody(p65) (Cat No.8242) and Anti-AKT (Cat No.4060) were purchased from Cell Signaling Technology (USA). DAB detection kit (Polymer) (PV6000-D) was purchased from Thermo Fisher Scientific (USA). DMSO (Cat No.3483C285), DTT (Cat No.0281), TEMED (Cat No.0761), and Tween-20 (Cat No.0777) were purchased from Sigma-Aldrich LLC(USA). BCA Protein Assay Kit (Cat No.02912E) were purchased from Jiangsu Cowin Biotech Co., Ltd. (China). Goat anti-mouse IgG (H+L), HRP (Cat No.115-035-003), goat anti-rabbit IgG (H+L) and HRP (Cat No.111-035-003) were purchased from Jackson Immuno Research laboratories. Inc (USA). ECL (WBKLS0500) was purchased from Sigma-Aldrich Co., Ltd. (USA). Rat IL-1 β ELISA Kit (Lot No.1229170721), Rat MCP-1 ELISA Kit (Lot No.0119180705), Rat TNF- α ELISA Kit (Lot No.0105180709) and Rat IL-6 ELISA Kit (Lot No.1229170724) were purchased from RayBiotech Life, Inc. (USA). Aspartate Aminotransferase (Cat No. AST/GOT) Activity Assay Kit (Reitman-Frankel Method) (Cat No.C010-1), Creatine kinase (CK) Activity Assay Kit (Cat No.A032), Lactate Dehydrogenase (LDH) Activity Assay Kit (Cat No.A020-2) were purchased from Nanjing Jiancheng Bioengineering Institute(China). Pentobarbital Sodium (Lot No.2017050505) was purchased from Shanghai Yiji Industrial Co., Ltd. (China)

Statistical analysis

All data are expressed as mean \pm standard error of the mean. Statistical software uses SPSS20.0 statistical data. The T-test is used for comparison between two groups, and analysis of variance (ANOVA) is used for comparison of three or more groups. *P* values less than 0.05 were considered significant. GraphPad Prism 9.0 software was used for statistical data, and the level of significance is indicated in the legend.

Results

Qualitative and quantitative analysis of SYI

In this study, qualitative and quantitative analysis of the main components in SYI was carried out to provide component and content information for subsequent in vitro pharmacological studies. Firstly, the mass spectrometry characteristics of the possible standards were studied, and a highly sensitive analysis method was constructed. Then, the chromatographic conditions were explored to

clarify which components were contained. On this basis, the qualitative analysis results were confirmed by high-performance liquid chromatography. According to literature reports and preliminary research, the objects to be analyzed include quercetin, hesperidin, rutin, luteolin, kaempferol, isorhamnetin, luteolingluco side, isoquercitrin, apigenin-7-O- β -D-glucoside, apiin, hydroxy safflower yellow A, anhydrosafflor yellow B, and scutellarin. MRM chromatograms of standard substance solution and safflower yellow pigment solution for injection are shown in Fig. 1A and B. Qualitative experimental results show that SYI mainly contains hydroxy safflower yellow A, and also contains a very small amount of anhydrosafflor yellow B and hesperidin (Fig. 1C). Moreover, quantitative analysis showed that the content of hydroxy safflower yellow A in safflower yellow for injection was about 103%, which could be because SYI mainly contains hydroxy safflower yellow A and the content is very high and the standard product may be insufficient purity, so the calculation results in more than 100% of the component to be tested. Chromatogram of the blank solution, reference solution and sample (UV403) were shown in Fig. 1D.

Effects of SYI on the pathological changes of myocardial tissue in rats with ischemia-reperfusion injury

In order to confirm the myocardial protective effect of SYI, the pathological changes of rat myocardial tissue were measured by HE staining. HE staining in sham group was neat and orderly, with no degeneration and necrosis of cells and no obvious inflammation in the interstition. In I/R group, myocardial tissue arrangement was disordered, myocardial cell edema and degeneration, interstitial edema, vascular proliferation, and expansion. After HBS and SYI treatment, myocardial tissue was arranged in an orderly manner, with mild edema and degeneration of local myocardial cells, mild interstitial edema, and a small amount of blood vessel proliferation and dilation (Fig. 2A).

Effects of SYI on myocardial ischemia area in rats with ischemia-reperfusion injury

Considering the changes in myocardial tissue after ischemia, the ischemic areas from each group were calculated and compared in the study. The percentage of myocardial ischemia area in I/R group was significantly increased ($P < 0.001$) when compared with the sham operation group. Compared with I/R group, the percentage of myocardial ischemic area were significantly decreased after the treatment of HBS and SYI ($P < 0.01$, $P < 0.05$), as shown in Fig. 2B.

Effects of SYI on serum myocardial enzyme activity in rats with ischemia-reperfusion injury

Further, in order to figure out the effect of SYI on serum myocardial enzyme activity, we examined the contents of AST, LDH and CK. Compared with sham group, the levels of serum of AST, LDH and CK in I/R group were significantly increased ($P < 0.01$). Compared with I/R group, the levels of serum of AST, LDH and CK were significantly decreased in I/R+HBS, I/R+SYI-H and I/R+SYI-M group ($P < 0.01$, $P < 0.05$). However, the levels of serum of AST, LDH and CK also decreased in the I/R+SYI-L group, but the difference was not statistically significant (Fig. 2C).

Effects of SYI on serum inflammatory factors in rats with ischemia-reperfusion injury

To determine whether SYI treatment can interfere with inflammatory factors induced by I/R in the myocardium, the serum was examined for the levels of TNF- α , IL-6, MCP-1 and IL-1 β . Compared with the sham operation group, the levels of inflammatory factors were significantly increased in I/R group ($P < 0.01$). Compared to I/R group, the content of TNF- α , IL-6 MCP-1 and IL-1 β were significantly decreased ($P < 0.01$, $P < 0.05$). SYI treatment reversed the elevation of inflammatory factors due to I/R, except in the SYI-L group. (Fig. 3A).

Effects of SYI on the expression of inflammation related proteins in myocardial tissue of rats with ischemia-reperfusion injury

To further explore the molecular mechanism of SYI's cardioprotective action, we examined the inflammation related proteins levels of Caspase-1, NLRP3, TLR4 and NF- κ B (p65). The result suggested that the expression levels of inflammation related proteins in the myocardial tissue of the rats in I/R group were significantly increased ($P < 0.01$). SYI and HBS treatment reversed the expression of inflammatory proteins, except for NLRP3 in the SYI-L group ($P < 0.01$, $P < 0.05$) (Fig. 3B).

Effects of SYI on the morphology of myocardial tissue cells in rats with ischemia-reperfusion injury

Interestingly, when we observed cell morphology with transmission microscopy, something new was discovered. Compared with the sham-operated group, the cell volume of the myocardial tissue of the rats in I/R group was reduced, the chromatin was condensed and marginalized, the nuclear membrane was lysed, and the surrounding mitochondria were dissolved, which are the manifestations of apoptosis. The I/R+SYI group did not have obvious cell volume reduction, the chromatin was normal, and the surrounding mitochondria were relatively intact (Fig. 4A). What's more important, a double or multi-layered vacuole-like structure, which contains

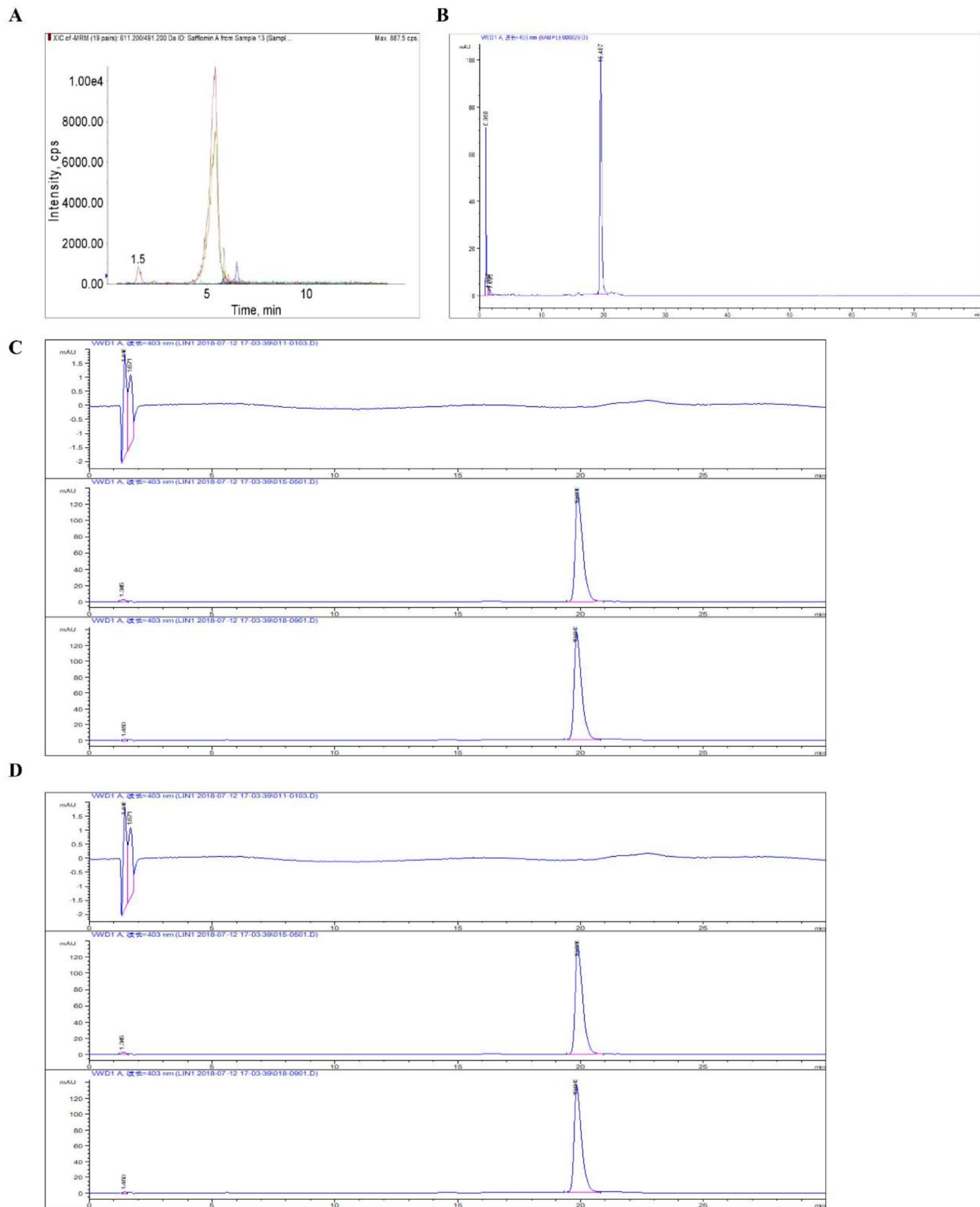


Fig. 1 Qualitative and quantitative analysis of SYI. **(A)** MRM chromatogram of standard substance solution. **(B)** MRM chromatogram of safflower yellow pigment solution for injection. **(C)** HPLC chromatogram of safflower yellow pigment solution for injection. **(D)** chromatogram of blank solution, reference solution and sample (UV403)

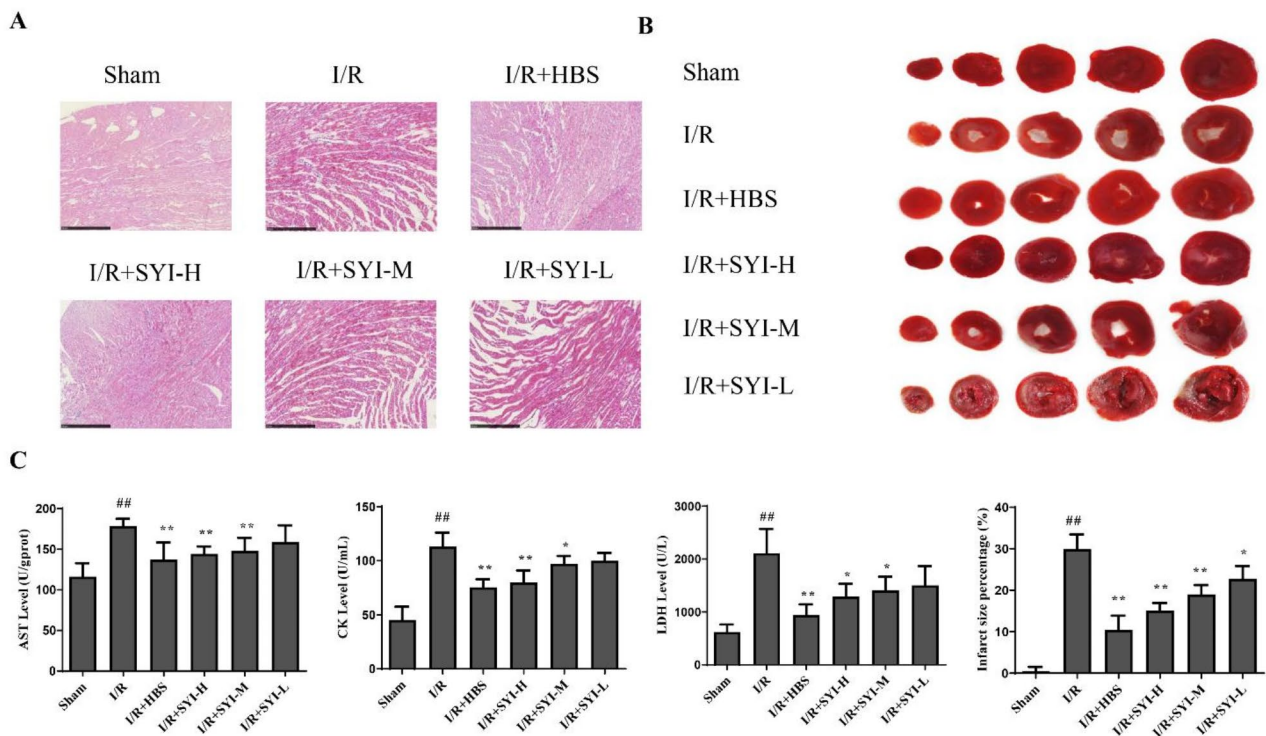


Fig. 2 Protective effect of SYI on myocardial tissue in rats with myocardial ischemia-reperfusion injury. **(A)** Influence of SYI on the pathological changes of myocardial tissue in rats with myocardial ischemia-reperfusion injury (100 \times , Scale:500 μ m). **(B)** Influence of SYI on myocardial infarction area percentage in rats with myocardial ischemia-reperfusion injury. **(C)** Influence of SYI on serum AST, LDH and CK levels in rats with myocardial ischemia-reperfusion injury. Sham, sham-operated group; I/R, ischemia-reperfusion group; HBS, hebeishuang group; I/R+SYI-L, I/R+SYI-low dose group; I/R+SYI-M, I/R+SYI-medium-dose group; I/R+SYI-H, I/R+SYI-high-dose group. Compared with the sham group, ^{##} $P < 0.01$; Compared with the model group, ^{**} $P < 0.01$, ^{*} $P < 0.05$

single or multiple mitochondrial cytoplasmic components, appeared in the I/R + SYI group, whose phenomena are typical manifestations of autophagy (Fig. 4B).

Effects of SYI on apoptosis related proteins in myocardial tissue of rats with ischemia-reperfusion injury

To further determine the relationship between SYI and apoptosis in myocardial tissue of ischemia-reperfusion injury rats, we next evaluated the apoptosis related proteins levels of Bcl-2, Bax, Caspase-3 and the rate of Bcl/Bax. The level of Bcl-2 and the rate of Bcl-2/Bax in the myocardial tissue of the rats in I/R group were significantly decreased ($P < 0.01$), and the protein expressions of Bax and Caspase-3 were significantly increased ($P < 0.01$). However, after HBS and SYI treatment, the expressions of Bcl-2/Bax and Bcl-2 were significantly increased, but the expressions of Caspase-3 and Bax protein were significantly decreased ($P < 0.01$, $P < 0.05$) (Fig. 5).

Effects of SYI on the expression of autophagy related proteins in myocardial tissue of rats with ischemia-reperfusion injury

Subsequently, we further confirm whether SYI can influence the autophagy of myocardial tissue after

ischemia-reperfusion injury, we examined the protein expressions of PI3K, Akt, mTOR, LC3-I, LC3-II and p62/SQSTM1. The results suggest the expressions of PI3K, Akt, mTOR and LC3-II in the myocardial tissue were significantly increased ($P < 0.01$, $P < 0.05$), whereas no significant differences in p62/SQSTM1 and LC3-I were found between Sham group and I/R group. However, in the I/R + SYI-H and I/R + HBS group, the protein expressions of PI3K, Akt, mTOR, LC3-I, and p62/SQSTM1 were significantly down-regulated ($P < 0.01$), the expression of LC3-II and LC3-II/LC3-I was significantly increased ($P < 0.01$) (Fig. 6).

Effects of SYI on the cell viability of OGD/R injured HUVECs

To further verify that SYI protects cardiomyocytes after ischemia-reperfusion by affecting autophagy, we performed cell experiments containing autophagy inhibitors. The cell viability in the OGD/R group was significantly decreased ($P < 0.01$). Compared with the OGD/R group, the cell viability in SYI group decreased ($P < 0.05$, $P < 0.01$), as shown in Fig. 7A. Furthermore, the cell volume was normal and cell nucleus was intact in the OGD/R group. However, the OGD/R+SYI group had more double-layer membrane structures, reduced cell

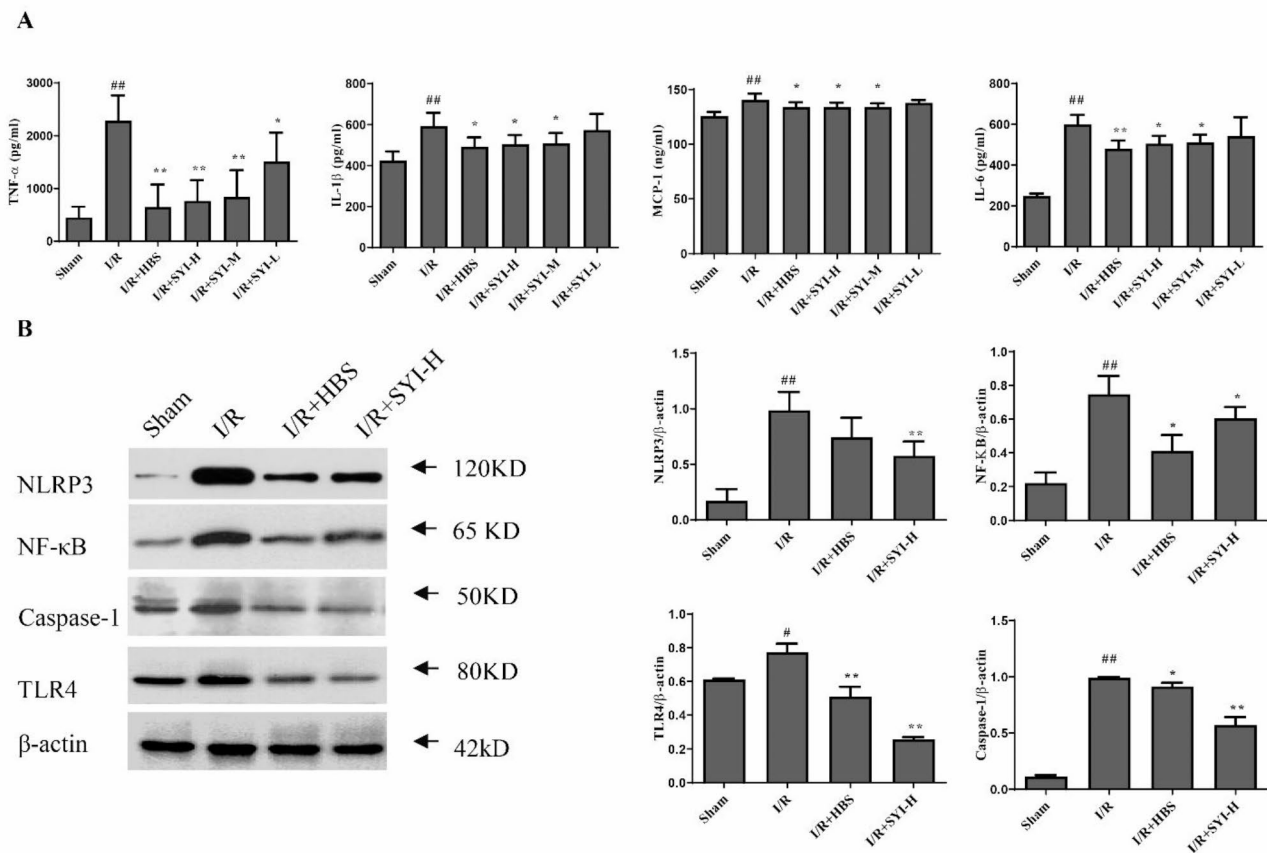


Fig. 3 Influence of SYI on serum inflammatory factors and inflammatory proteins in rats with myocardial ischemia-reperfusion injury. **(A)** Influence of SYI on serum inflammatory factors in rats with myocardial ischemia-reperfusion injury. **(B)** Effects of SYI on the expression of inflammatory proteins Caspase-1, NLRP3, TLR4 and NF- κ B (p65) in myocardial tissue of rats with myocardial ischemia-reperfusion injury. Sham, sham-operated group; I/R, ischemia-reperfusion group; HBS, hebeishuang group; I/R+SYI-L, I/R+SYI-low dose group; I/R+SYI-M, I/R+SYI-medium-dose group; I/R+SYI-H, I/R+SYI-high-dose group. Compared with the sham group, $^{##}P < 0.01$; Compared with the model group, $^{**}P < 0.01$, $^{*}P < 0.05$

volume, shrunken cell membranes, and no intact nucleus. The OGD/R + SYI + CQ group reversed these phenomena (Fig. 7B).

Effects of SYI on inflammatory factors in OGD/R injured HUVECs

To further confirm the relationship between SYI and inflammatory factors, we detected the contents of IL-1 β , IL-6, MCP-1 and TNF- α in OGD/R-injured HUVECs after adding an autophagy inhibitor. The contents of inflammatory factors were significantly increased in the OGD/R group ($P < 0.01$), but decreased in the OGD/R+SYI group ($P < 0.01$, $P < 0.05$). The contents of inflammatory factors were significantly increased in OGD/R+SYI+CQ group when compared with the OGD/R+SYI group (Fig. 7C).

Effects of SYI on inflammation related proteins in OGD/R injured HUVECs

We further examined the influence of SYI on the expression of inflammation-related proteins in OGD/R-injured HUVECs after adding an autophagy inhibitor. Compared with NC group, the protein expressions of Caspase-1, NLRP3, TLR4 and NF- κ B in the OGD/R group were significantly increased ($P < 0.01$). Compared with OGD/R group, the expressions of inflammation-related proteins in OGD/R+SYI group were significantly decreased ($P < 0.01$). Be different from OGD/R+SYI group, the expressions of NLRP3, TLR4 and NF- κ B in the OGD/R+SYI+CQ group were significantly increased ($P < 0.01$, $P < 0.05$), as shown in Fig. 8A.

Effects of SYI on autophagy related proteins in OGD/R injured HUVECs

Furthermore, in order to verify the mechanism of SYI on cardio protection, we examined the protein expressions of PI3K, p-Akt, mTOR, LC3-I and p62/SQSTM1.

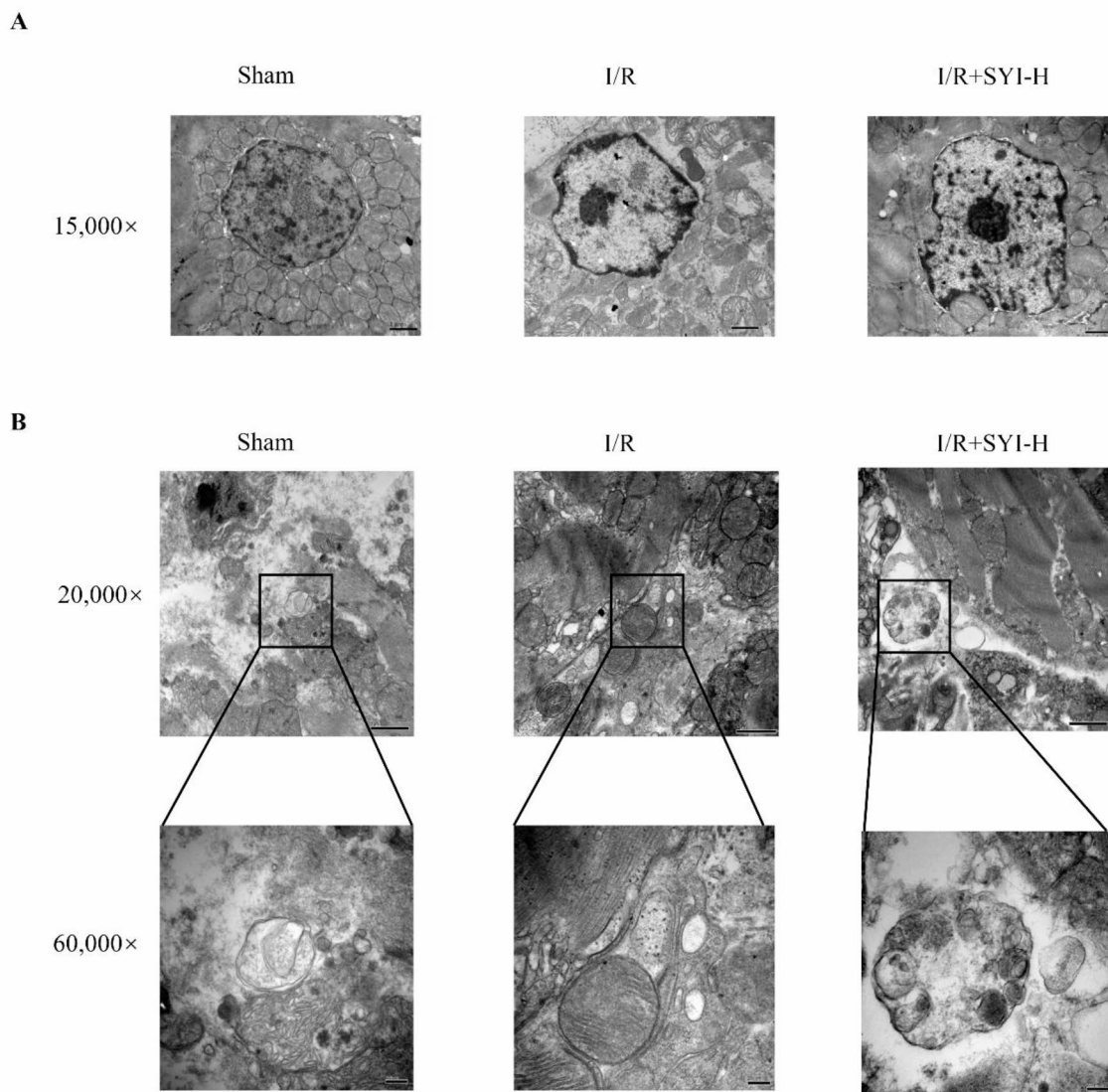


Fig. 4 Cell morphology of rat with myocardial ischemia-reperfusion injury under the transmission electron microscope. **(A)** Apoptosis of rat with myocardial ischemia-reperfusion injury under the transmission electron microscope. **(B)** Autophagy of rat with myocardial ischemia-reperfusion injury under a transmission electron microscope in I/R+SYI. Sham, sham-operated group; I/R, ischemia-reperfusion group; I/R+SYI-H, I/R+SYI-high dose group

Compared with NC group, the protein expressions of PI3K, p-Akt and mTOR were significantly increased ($P < 0.01$), however, that wasn't a significant effect on the protein levels of LC3-I and p62/SQSTM1 in the OGD/R group. Compared with the OGD/R group, the expressions of autophagy related proteins were significantly decreased in the OGD/R+SYI group ($P < 0.01$). However, LC3-II/LC3-I were significantly decreased ($P < 0.01$) and the protein expressions PI3K, p-Akt, mTOR and p62/SQSTM1 were significantly increased in the OGD/R+SYI+CQ group ($P < 0.01$, $P < 0.05$) (Fig. 8B).

Discussion

During the onset and treatment of CAD, MIRI is an important factor that seriously affects the survival rate and long-term recovery of cardiac function after coronary revascularization [33–35]. Inflammation is a key pathological mechanism involved in the process of MIRI, and the activation of the NLRP3 inflammasome and its downstream signaling molecules is the key link in inducing the inflammatory response of MIRI. Relevant studies suggest that inflammasome NLRP3 can be activated by the production of intracellular ROS, except activated by a variety of pathogen-related molecular pattern receptors and endogenous danger signals [36, 37]. Therefore, regulating the activation of NLRP3 inflammasome can

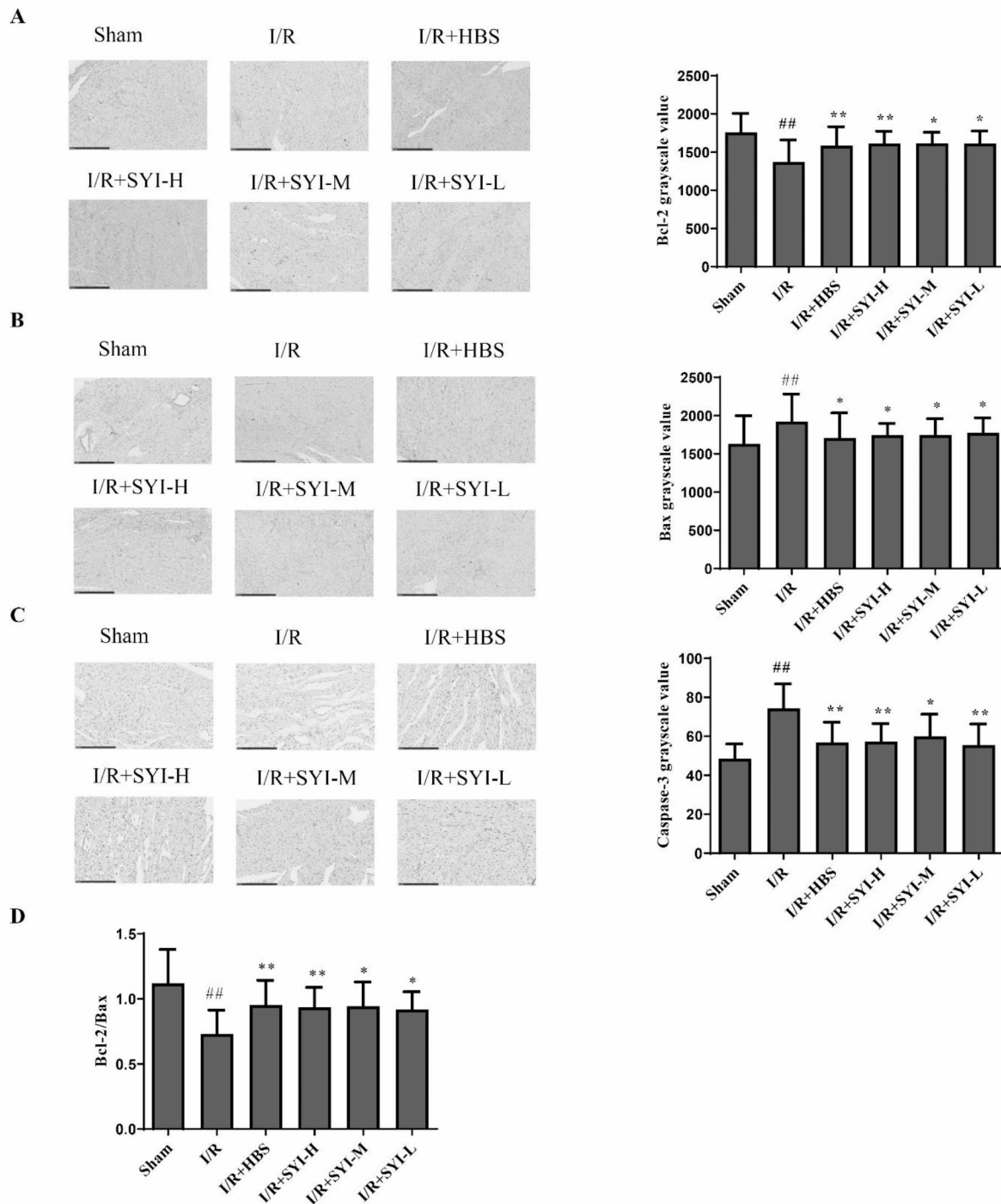


Fig. 5 Effects of SYI-L on apoptosis in rats with myocardial ischemia-reperfusion injury. **(A)** The levels of Bal-2 in cardiac tissues were measured by western blot. **(B)** The levels of Bax in cardiac tissues were measured by western blot. **(C)** The levels of Caspase-3 in cardiac tissues were measured by western blot. **(D)** The levels of Bal-2/Bax in cardiac tissues were measured. Sham, sham-operated group; I/R, ischemia-reperfusion group; HBS, hebeishuang group; I/R+SYI-L, I/R+SYI-low dose group; I/R+SYI-M, I/R+SYI-medium-dose group; I/R+SYI-H, I/R+SYI-high-dose group. Compared with the sham group, ^{##}*P*<0.01; Compared with the model group, ^{**}*P*<0.01, ^{*}*P*<0.05

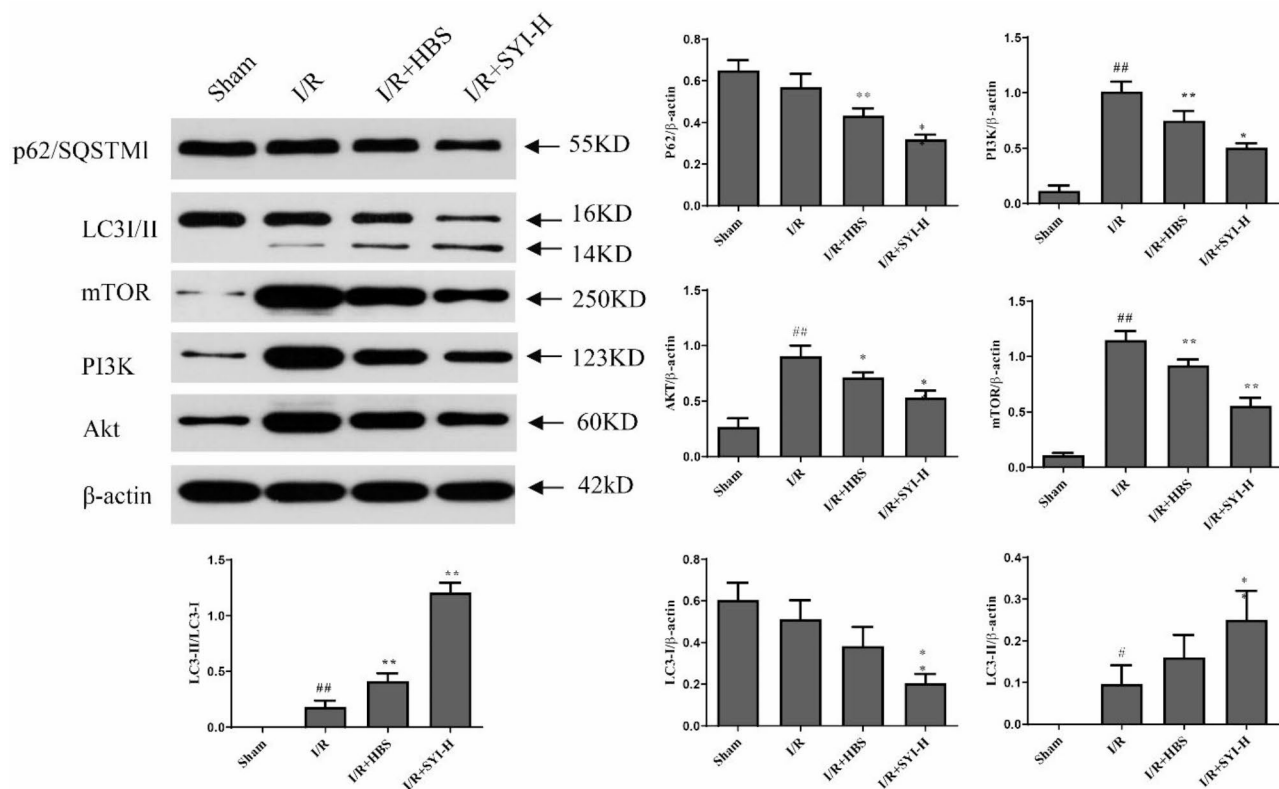


Fig. 6 Effects of SYI-H on autophagy in rats with myocardial ischemia-reperfusion injury. Sham, sham-operated group; I/R, ischemia-reperfusion group; I/R+SYI-H, I/R+SYI-high dose group. Compared with the sham group, ##*P*<0.01; Compared with the model group, **P*<0.01, **P*<0.05

control the occurrence of inflammation in the body, which is of great significance for the prevention and control of MIRI [38–41].

In this study, after clarifying the content and composition of SYI by mass spectrometry, we adopt a rat model of acute MIRI, so as to detect whether SYI has a protective effect on MIRI in rats. These results, after detecting changes in myocardial ischemia area, myocardial tissue pathology and HE staining, have found that SYI can improve myocardial histopathological response, reduce vascular proliferation and cell edema, reduce the area percentage of myocardial ischemic and inflammatory infiltration in rats. What's more, the appearance of inflammatory infiltration in HE staining suggests that inflammatory response plays an important role in ischemia-reperfusion injury. The reductions in the levels of serum inflammatory factors TNF- α , IL-6, MCP-1, IL-1 β and serum myocardial enzymes CK, LDH and AST in rats were found, which suggested that the treatment of SYI, after MIRI in rats, can alleviate the myocardial cell damage. Further, the results of inflammatory response-related proteins showed that SYI could reduce the protein expression of TLR4, NF- κ B (p65), NLRP3 and Caspase-1. Our results suggest that SYI can inhibit the activation of the TLR4/NF- κ B (p65) pathway and NLRP3

inflammasome pathway, thereby protecting the injured myocardium after MIRI in rats by inhibiting the inflammatory response.

Apoptosis and inflammation are closely related. On the one hand, apoptosis suppresses inflammation and apoptotic vesicles are phagocytosed without activating the immune system. Apoptosis maintains tissue homeostasis, as in embryonic development, and apoptosis induced by regulatory T cells also suppresses inflammatory factors [42–46]. On the other hand, inflammation induces apoptosis, and inflammatory mediators such as reactive oxygen species and TNF- α activate apoptotic pathways, and persistent inflammatory stimuli also affect tissues [47–52]. Though transmission electron microscope observation, we found that some cells showed the characteristics of apoptosis, such as cell size reduction, nuclear chromatin condensation, nuclear membrane lysis and the dissolution of surrounding mitochondria. This suggests that there is a close relationship between apoptosis and autophagy after acute MIRI in rats. Therefore, in order to explore whether SYI affects acute MIRI by regulating apoptosis, the protein expression levels of Bax, Bcl2, and Caspase-3 in the apoptosis pathway were detected in the further study. Bax can promote apoptosis, while Bcl-2 can antagonize apoptosis. Bax/Bcl-2 ratio

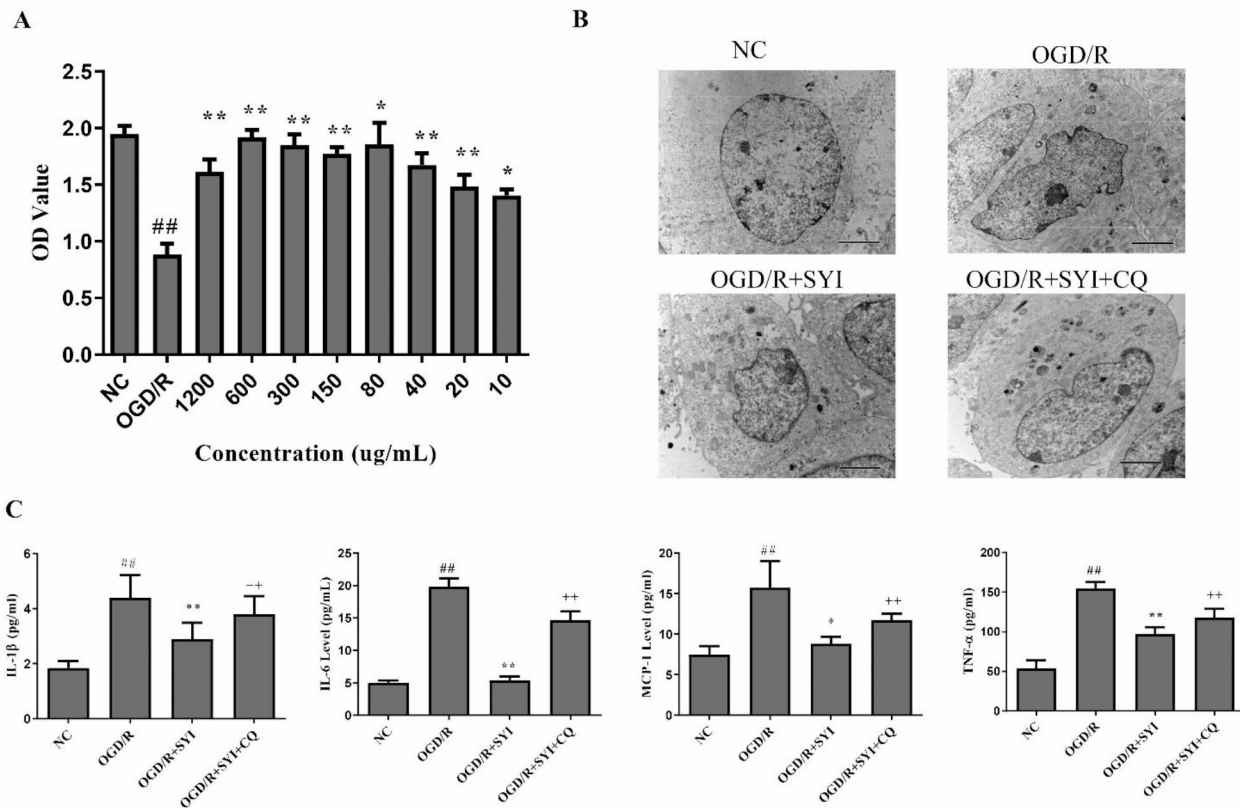


Fig. 7 The effect of SYI on the cell viability of OGD/R-injured HUVECs added with an autophagy inhibitor. **(A)** Relationship between cell activity and SYI concentration. **(B)** Cell morphology under the transmission electron microscope. **(C)** Influence of autophagy inhibitor on serum inflammatory factors in rats with OGD/R injury. NC, normal control group; OGD/R, Oxygen-Glucose Deprivation/Reoxygenation group; OGD/R+SYI+CQ, OGD/R+SYI+Chloroquine. Compared with the normal control group, $^{##}P < 0.01$; Compared with the OGD/R group, $^{**}P < 0.01$, $^{*}P < 0.05$; Compared with the OGD/R+SYI-L group, $^{++}P < 0.01$

affects the survival of cardiomyocytes. Increased Bax and decreased Bcl-2 can open mitochondrial permeability transition pores and exacerbate cytochrome C release, ultimately triggering the activation of caspase-7 and caspase-3 leading to apoptosis. Our results confirmed that SYI can reduce the ratio of Bax/Bcl-2 by down-regulating Bax and up-regulating Bcl-2, and can reduce the increase of caspase-3 activity caused by H/R, thereby reducing cell apoptosis.

Previous studies have found that autophagy was one important factor to promote the activation of the NLRP3 inflammasome [53]. The PI3K/Akt/mTOR pathway is one of the currently known inhibitory pathways in the regulation of autophagy [54]. Our results further confirmed that PI3K, Akt, mTOR, p62/SQSTM1 proteins were down-regulated and LC3 protein expression was up-regulated in MIRI rats after SYI treatment. Consequently, our results were suggested that SYI may reduce the NLRP3 inflammasome by blocking or attenuating PI3K/Akt/mTOR pathway signaling, up-regulating the

expression of autophagy-related proteins, in order to protect the myocardial tissue by promoting autophagy.

Further, we explored the interrelationship between autophagy and inflammation in SYI-induced MIRI in rats. In the heart, inflammatory factors are mainly secreted by endothelial cells, but not by cardiomyocytes, so we selected endothelial cells for subsequent experiments [55]. Through the OGD/R injury model of endothelial cells, we found that SYI can inhibit the release levels of inflammatory factors TNF- α , IL-6, MCP-1, and IL-1 β , but this inhibitory effect was significantly reduced after the addition of autophagy inhibitor CQ. In addition, CQ could also reverse the decreased expression levels of inflammation-related proteins such as TLR4, NF- κ B (p65), NLRP3, and Caspase-1 induced by SYI after OGD/R. Activation of TLR4 can induce downstream NF- κ B, and the activation of NF- κ B mediates the activation of the NLRP3 inflammasome, resulting in the expression of Caspase-1. PI3K is an intracellular phosphatidylinositol kinase, which is a key molecule in various life activities, and Akt is a downstream signaling

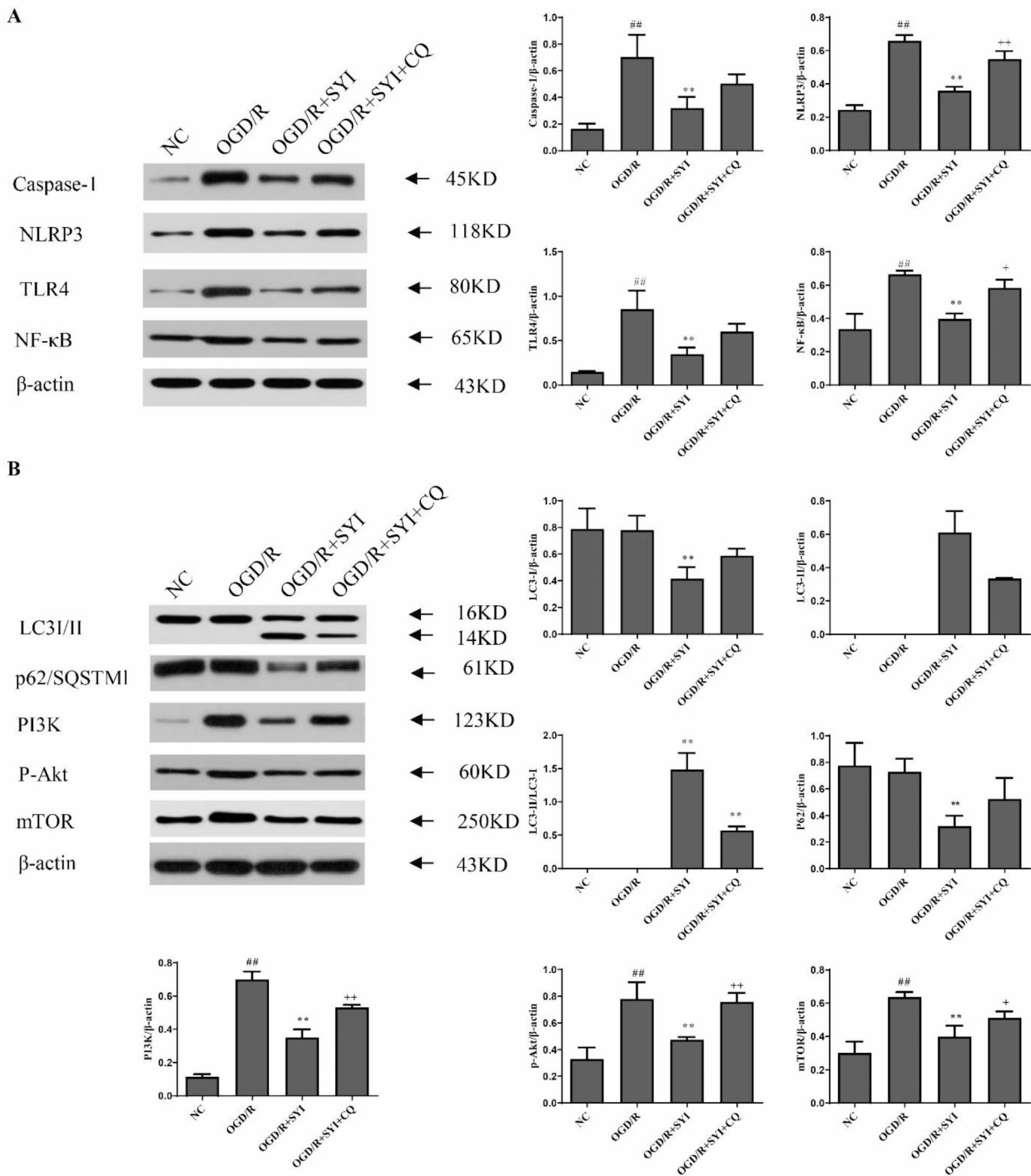


Fig. 8 The effect of SYI on inflammation-related proteins and autophagy-related proteins in OGD/R-injured HUVECs added with autophagy inhibitors. **(A)** The effect of SYI on inflammation-related proteins in OGD/R-injured HUVECs with autophagy inhibitor added. **(B)** The effect of SYI on autophagy-related proteins in OGD/R-injured HUVECs added with an autophagy inhibitor. NC, normal control group; OGD/R, Oxygen-Glucose Deprivation/Reoxygenation group; OGD/R+SYI+CQ, OGD/R+SYI+Chloroquine. Compared with the normal control group, ##*P*<0.01; Compared with the OGD/R group, ***P*<0.01, **P*<0.05; Compared with the OGD/R+SYI-L group, ++*P*<0.01

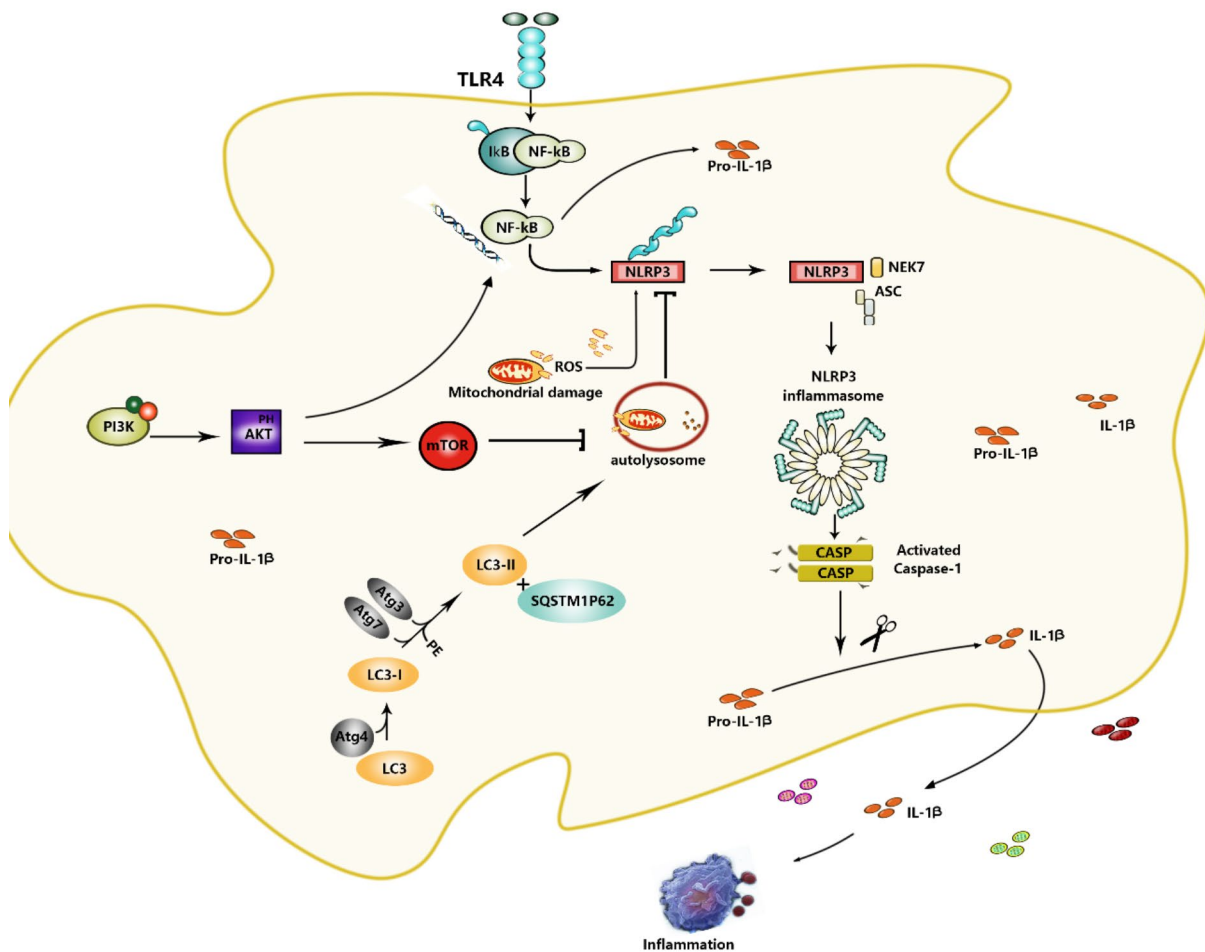


Fig. 9 Regulation of NLRP3 inflammasome-related signaling pathways

molecule of PI3K [56]. Activated PI3K inhibits autophagy lysosome production by acting on and phosphorylating Akt, which in turn activates the downstream molecule mTOR [57]. Autophagy lysosomes inhibit the accumulation of ROS, thereby reducing the activation of NLRP3 inflammatory vesicles [58]. Our results suggested that SYI inhibited PI3K/Akt/mTOR and promotes autophagy lysosome production, which in turn promoted autophagy and inhibited NLRP3 inflammatory vesicle-mediated inflammatory responses.

In summary, we demonstrated that SYI had significant anti-inflammatory and protective effects on MIRI in rats, which related to the regulation of NLRP3 inflammasome. There may be two signaling pathways that SYI regulates the NLRP3 inflammasome: On the one hand, SYI can inhibit or block the TLR4/NF- κ B (p65) pathway, thereby reducing the activation of the NLRP3 inflammasome. On the other hand, SYI can block or attenuate PI3K/Akt/

mTOR signaling pathway, increase autophagy lysosomes, reduce ROS accumulation and its mediated NLRP3 inflammasome activation (Fig. 9).

Conclusion

In conclusion, we demonstrated that SYI can promote myocardial tissue autophagy in a rat model of acute MIRI, as well as reduce the myocardial inflammatory response. On the one hand, SYI can inhibit the initiation of TLR4/NF- κ B, thereby reducing the activation of NLRP3 inflammasome, in order to inhibit inflammation response to protect damaged myocardium. On the other hand, SYI can inhibit NLRP3 inflammasome activation by blocking or attenuating PI3K/Akt/mTOR pathway to promote autophagy-lysosome production in order to promote autophagy protect damaged myocardium.

Supplementary Information

The online version contains supplementary material available at <https://doi.org/10.1186/s12906-025-04747-8>.

Supplementary Material 1

Supplementary Material 2

Acknowledgements

Thanks to the National Natural Science Foundation of China for the funding support for this project.

Author contributions

Xiao Han, Qiong Zhang and Jianhua Fu supervised the whole project. Lingmei Li and Ce Cao performed the major research and wrote the manuscript in equal contributions. Hao Guo, Li Lin, Lei Li, Gaojie Xin, Zixin Liu and Shujuan Xu provided their professional expertise.

Funding

This work was supported by the Science and Education Project of Suzhou (KJXW2023078), National Natural Science Foundation of China (81673817, 81774145), Beijing Natural Science Foundation (7172191) and National Science Fund for Distinguished Young Scholars of China (81503292).

Data availability

All data generated or analyzed during this study are included in this article and its supplementary information files.

Declarations

Ethics approval and consent to participate

Animal feeding and experimental operations were performed at the Experimental Animal Center of Xiyuan Hospital [SYXK (Beijing) 2018-0018]. The treatment of experimental animals strictly followed the principles of "reduction, substitution, and optimization" and was provided humanely. The Ethics Committee of Xiyuan Hospital approved the study (Number 2021XLC037). All methods are reported in accordance with ARRIVE guidelines for the reporting of animal experiments. All methods were performed in accordance with the relevant guidelines and regulations.

Consent for publication

Not Applicable.

Competing interests

The authors declare no competing interests.

Author details

¹Kunshan Hospital of Chinese Medicine, Kunshan, China

²Institute of Basic Medical Sciences of Xiyuan Hospital, Beijing Key Laboratory of Chinese Materia Pharmacology, China Academy of Chinese Medical Sciences, National Clinical Research Center of Traditional Chinese Medicine for Cardiovascular Diseases, Beijing, China

Received: 19 March 2023 / Accepted: 6 January 2025

Published online: 09 January 2025

References

1. Yang Y, et al. Acetylation, ferroptosis, and their potential relationships: implications in myocardial ischemia-reperfusion injury. *Am J Med Sci*. 2023;366(3):176–84.
2. Rabinovich-Nikitin I, Kirshenbaum LA. Circadian regulated control of myocardial ischemia-reperfusion injury. *Trends Cardiovasc Med*. 2024;34(1):1–7.
3. Buja LM. Myocardial ischemia and reperfusion injury. *Cardiovasc Pathol*. 2005;14(4):170–5.
4. Wang J, et al. Recent advances in nanomedicines for imaging and therapy of myocardial ischemia-reperfusion injury. *J Control Release*. 2023;353:563–90.
5. Zhang P, et al. Role of Hydrogen Sulfide in Myocardial Ischemia-Reperfusion Injury. *J Cardiovasc Pharmacol*. 2021;77(2):130–41.
6. Algoet M, et al. Myocardial ischemia-reperfusion injury and the influence of inflammation. *Trends Cardiovasc Med*. 2023;33(6):357–66.
7. Li T, et al. Resveratrol protects against myocardial ischemia-reperfusion injury via attenuating ferroptosis. *Gene*. 2022;808:145968.
8. Wang K, et al. Role of epigenetic regulation in myocardial ischemia/reperfusion injury. *Pharmacol Res*. 2021;170:105743.
9. Shen Y, et al. Involvement of Nrf2 in myocardial ischemia and reperfusion injury. *Int J Biol Macromol*. 2019;125:496–502.
10. Chang C, et al. Mesenchymal stem cell-derived exosomal noncoding RNAs as alternative treatments for myocardial ischemia-reperfusion injury: current status and future perspectives. *J Cardiovasc Transl Res*. 2023;16(5):1085–98.
11. Zhang D, et al. Research Progress on the mechanism and treatment of Inflammatory Response in Myocardial Ischemia-Reperfusion Injury. *Heart Surg Forum*. 2022;25(3):E462–8.
12. Hong JJ et al. Off-label uses of TNF- α inhibitors and IL-1/2/3 inhibitors in dermatology. *Dermatol Online J*. 2021;27(11).
13. Skiniotis G, et al. Signaling conformations of the tall cytokine receptor gp130 when in complex with IL-6 and IL-6 receptor. *Nat Struct Mol Biol*. 2005;12(6):545–51.
14. Weber A, Wasiliew P, Kracht M. Interleukin-1 beta (IL-1 beta) processing pathway. *Sci Signal*. 2010;3(105):cm2.
15. Björner K et al. High iNOS and IL-1 β immunoreactivity are features of colitis-associated colorectal cancer tumors, but fail to predict 5-year survival. *Ups J Med Sci*. 2023;28.
16. Li S et al. NLRP3/caspase-1/GSDMD-mediated pyroptosis exerts a crucial role in astrocyte pathological injury in mouse model of depression. *JCI Insight*. 2021;6(23):e146852.
17. Bambouskova M, et al. Itaconate confers tolerance to late NLRP3 inflammasome activation. *Cell Rep*. 2021;34(10):108756.
18. Juan VR, et al. Reperfusion therapy with recombinant human relaxin-2 (sere-laxin) attenuates myocardial infarct size and NLRP3 inflammasome following ischemia/reperfusion injury via eNOS-dependent mechanism. *Cardiovascular Res*. 2017;113(6):609–19.
19. Jianwei X et al. Economic evaluation of safflower yellow injection for the treatment of patients with stable angina pectoris in China: a cost-effectiveness analysis. *Journal of alternative and complementary medicine (New York, N.Y.)*. 2018;24(6):564–569.
20. X ZM et al. Effect of hydroxy safflower yellow A on myocardial apoptosis after acute myocardial infarction in rats. *Genet Mol Research: GMR*. 2015;14(2):3133–41.
21. ZhouMingxue. The effect of hydroxy safflower yellow A on inflammatory reaction in myocardium of the rats after acute myocardial infarction. *Afr J Pharm Pharmacol*. 2013;7(12).
22. Ye J-x et al. Hydroxysafflor yellow A inhibits hypoxia/reoxygenation-induced cardiomyocyte injury via regulating the AMPK/NLRP3 inflammasome pathway. *Int Immunopharmacol*. 2020;82(C):106316.
23. Li LM, et al. Protective effect of safflower yellow injection against rat MIRI by TLR-NF- κ B inflammatory pathway. *Zhongguo Zhong Yao Za Zhi*. 2019;44(12):2566–71.
24. Lyu X et al. Safflower yellow and its main component hydroxysafflor yellow A alleviate hyperleptinemia in diet-induced obesity mice through a dual inhibition of the GIP-GIPR signaling axis. *Phytother Res*. 2023;38(10):4940–4956.
25. Liu Y, et al. Safflower yellow for injection enhances anti-coagulation of warfarin in rats: implications in pharmacodynamics and pharmacokinetics. *Xenobiotica*. 2024;54(2):75–82.
26. Aguiar ACC, et al. Chloroquine analogs as antimalarial candidates with potent in vitro and in vivo activity. *Int J Parasitol Drugs Drug Resist*. 2018;8(3):459–64.
27. Ferreira PMP, et al. Chloroquine and hydroxychloroquine in antitumor therapies based on autophagy-related mechanisms. *Pharmacol Res*. 2021;168:105582.
28. Varisli L, Cen O, Vlahopoulos S. Dissecting pharmacological effects of chloroquine in cancer treatment: interference with inflammatory signaling pathways. *Immunology*. 2020;159(3):257–78.
29. R SN et al. The effects of therapeutic sulfide on myocardial apoptosis in response to ischemia-reperfusion injury. *Eur J cardio-thoracic Surgery: Official J Eur Association Cardio-thoracic Surg*. 2008;33(5).
30. Dhote VV, Balaraman R. Gender specific effect of progesterone on myocardial ischemia/reperfusion injury in rats. *Life Sci*. 2007;81(3).

31. Hylde Z et al. Acute administration of n-3 rich triglyceride emulsions provides cardioprotection in murine models after ischemia-reperfusion. *PLoS ONE*. 2015;10(1).
32. Gangying H et al. Anti-inflammatory effect of B-type natriuretic peptide postconditioning during myocardial ischemia-reperfusion: involvement of PI3K/Akt signaling pathway. *Inflammation*. 2014;37(5).
33. Liu Z, et al. Shuangshen Ningxin formula attenuates cardiac microvascular ischemia/reperfusion injury through improving mitochondrial function. *J Ethnopharmacol*. 2024;323:117690.
34. Cao C, et al. Huoxin Pill reduces myocardial Ischemia Reperfusion Injury in rats via TLR4/NFκB/NLRP3 signaling pathway. *Chin J Integr Med*. 2023;29(12):1066–76.
35. Li L, et al. Investigation of the active ingredients of Shuangshen Ningxin Formula and the mechanism underlying their protective effects against myocardial ischemia-reperfusion injury by mass spectrometric imaging. *Phytomedicine*. 2024;123:155184.
36. Shao BZ, et al. NLRP3 inflammasome and its inhibitors: a review. *Front Pharmacol*. 2015;6:262.
37. Fu J, Wu H. Structural mechanisms of NLRP3 Inflammasome Assembly and Activation. *Annu Rev Immunol*. 2023;41:301–16.
38. M AJ, et al. Redox regulation of NLRP3 inflammasomes: ROS as trigger or effector? *Antioxidants & redox signaling*. 2015;22:13.
39. Wang L, et al. NLRP3 inflammasome activation: a therapeutic target for cerebral ischemia-reperfusion Injury. *Front Mol Neurosci*. 2022;15:847440.
40. Zhao C, Zhao W. NLRP3 Inflammasome-A key player in antiviral responses. *Front Immunol*. 2020;11:211.
41. Kelley N et al. The NLRP3 inflammasome: an overview of mechanisms of activation and regulation. *Int J Mol Sci*. 2019;20(13):3328.
42. Vignola AM, et al. Apoptosis and airway inflammation in asthma. *Apoptosis*. 2000;5(5):473–85.
43. Xie G, et al. The dysregulation of miRNAs in epilepsy and their regulatory role in inflammation and apoptosis. *Funct Integr Genomics*. 2023;23(3):287.
44. van den Oever IA, et al. Endothelial dysfunction, inflammation, and apoptosis in diabetes mellitus. *Mediators Inflamm*. 2010;2010:p792393.
45. Sharma S, Kaufmann T, Biswas S. Impact of inhibitor of apoptosis proteins on immune modulation and inflammation. *Immunol Cell Biol*. 2017;95(3):236–43.
46. Park HH. PYRIN domains and their interactions in the apoptosis and inflammation signaling pathway. *Apoptosis*. 2012;17(12):1247–57.
47. Kang R, et al. Deoxynivalenol induced apoptosis and inflammation of IPEC-J2 cells by promoting ROS production. *Environ Pollut*. 2019;251:689–98.
48. Doran AC, Yurdagul A Jr, Tabas I. Efferocytosis in health and disease. *Nat Rev Immunol*. 2020;20(4):254–67.
49. Onishi Y, Tanimoto Y, Kizaki H. Inflammation and apoptosis. *Bull Tokyo Dent Coll*. 1997;38(2):65–76.
50. Vringer E, Tait SWG. Mitochondria and cell death-associated inflammation. *Cell Death Differ*. 2023;30(2):304–12.
51. Bertheloot D, Latz E, Franklin BS. Necroptosis, pyroptosis and apoptosis: an intricate game of cell death. *Cell Mol Immunol*. 2021;18(5):1106–21.
52. Abdul Ghani MA et al. Role of terpenophenolics in modulating inflammation and apoptosis in Cardiovascular diseases: a review. *Int J Mol Sci*. 2023;24(6):5339
53. Fabio DL, Paolo B. Modulation of mitochondrial permeability transition in ischemia-reperfusion injury of the heart. *Advantages and limitations. Current medicinal chemistry*; 2015;22(20):2480-7
54. You-Tong W et al. Activation of the PI3K-Akt-mTOR signaling pathway promotes necrotic cell death via suppression of autophagy. *Autophagy*. 2009;5(6):824-34.
55. Amersfoort J, Eelen G, Carmeliet P. Immunomodulation by endothelial cells - partnering up with the immune system? *Nat Rev Immunol*. 2022;22(9):576–88.
56. Thapa N, et al. Phosphatidylinositol-3-OH kinase signalling is spatially organized at endosomal compartments by microtubule-associated protein 4. *Nat Cell Biol*. 2020;22(11):1357–70.
57. Kim JH, et al. Mitochondrial ROS-derived PTEN oxidation activates PI3K pathway for mTOR-induced myogenic autophagy. *Cell Death Differ*. 2018;25(11):1921–37.
58. Redza-Dutordoir M, Averill-Bates DA. Interactions between reactive oxygen species and autophagy: special issue: death mechanisms in cellular homeostasis. *Biochim Biophys Acta Mol Cell Res*. 2021;1868(8):119041.

Publisher's note

Springer Nature remains neutral with regard to jurisdictional claims in published maps and institutional affiliations.